

Electronic Supplementary Material for:

Sensing Mechanism of Ethanol and Acetone at Room Temperature by SnO₂ Nanocolumns Synthesized by Aerosol Routes: DFT and MD Simulations Compared to Experimental Results

Ahmed A. Abokifa¹, Kelsey Haddad¹, John Fortner¹, Cynthia S. Lo¹, and
Pratim Biswas^{1,*}

¹ Department of Energy, Environmental and Chemical Engineering
Washington University in St. Louis,
St. Louis, MO 63130, USA

*Corresponding author: P. Biswas (pbiswas@wustl.edu).

Tel: +1-314-935-5548 Fax: +1-314-935-5464

Section S1. Testing the convergence of the k-points mesh

First, the convergence of the used k-point mesh is tested for the total energy of the relaxed structure for the bulk calculations of the rutile SnO₂ unit cell ($a=b=4.83 \text{ \AA}$, and $c=3.24 \text{ \AA}$ – [8 atoms]). The results show that sufficient accuracy is achieved with a $5 \times 5 \times 7$ mesh (only 0.46 meV/cell difference between the $5 \times 5 \times 7$ mesh and the higher density $7 \times 7 \times 9$ mesh).

Given the large size of the slab models $p(2 \times 2)$ - [105 atoms], a $3 \times 3 \times 1$ mesh is used for the (101) surface ($11.64 \text{ \AA} \times 9.66 \text{ \AA}$), and a $4 \times 2 \times 1$ mesh is used for the (110) surface ($6.49 \text{ \AA} \times 13.66 \text{ \AA}$). To test the convergence of the adsorption energy with the density of the k-point mesh, the energy for ethanol adsorption on the stoichiometric (101) surface is calculated using two higher mesh densities of $(5 \times 5 \times 1)$ and $(7 \times 7 \times 1)$ in addition to the employed density of $(3 \times 3 \times 1)$. The results show that the total energy is almost insensitive to the increase in the mesh density beyond $(3 \times 3 \times 1)$, and the adsorption energy difference is only 0.14 meV (0.008% of E_{ads}) for the $(5 \times 5 \times 1)$ case and 0.12 meV (0.007% of E_{ads}) for the $(7 \times 7 \times 1)$ case. In addition, the difference in the calculated charge transfer is $(3.1\text{E-}5 \text{ e})$ for the $(5 \times 5 \times 1)$ and $(4.3\text{E-}5 \text{ e})$ for the $(7 \times 7 \times 1)$.

Section S2. Classical MD simulation for ethanol and acetone adsorption on Red(101)

To study the interactions between the surface and the adsorbates under ambient conditions for both a larger surface and a longer simulation period compared to AIMD, we perform classical force field molecular dynamics (FF-MD) simulations considering the canonical (NVT) ensemble. A Nose–Hoover thermostat is implemented to conduct constant temperature simulations at $T = 298$ K. All MD simulations are performed using LAMMPS within the Medea[®] software environment, with the PCFF forcefield. To appropriately represent the electrostatic interactions in the system, we use adjusted partial charges for the SnO₂ surface and the adsorbate molecules that are obtained from the charge analysis conducted at the quantum mechanical level with DFT. A time step of 1 femtosecond (fs) is used to integrate the equations of motion, and 100 picosecond (ps) trajectories are generated for all adsorbate–adsorbent systems for each simulation.

To simulate a large interface for surface interactions between SnO₂ and the adsorbate molecules in the conducted MD simulations, a simulation box consisting of 384 atoms (4 layers of Sn₃₂O₆₄) with surface dimensions of (23.3 Å × 19.3 Å) is used to represent the (101) SnO₂ surface facet, and a vacuum space of 40 Å is imposed above the surface. To create a reduced surface, eight bridging oxygen atoms are removed from the topmost layer, which is equivalent to one-half of all the exposed bridging oxygen atoms.

The adsorption of both ethanol and acetone on the reduced surface is studied for two different scenarios. The first scenario represents high O₂ concentration in the atmosphere, where twelve O₂ molecules (1.5X the number of surface oxygen defects) are first placed randomly at a distance from the surface, and the system's energy is minimized to ensure that oxygen molecules find stable adsorption sites on the surface. The second scenario is represents low O₂ concentration with only four O₂ molecules (0.5X the number of surface oxygen defects) are considered for pre-adsorption. Afterwards, for both scenarios, eight acetone (or ethanol) molecules are added to the system to investigate their binding to the surface in the presence of pre-adsorbed oxygen.

For the low O₂ case, all the simulated oxygen molecules adsorb at the oxygen vacancy sites in the optimized system. However, since the number of O₂ molecules is equal to half that of the oxygen vacancies, half the vacancy sites are still unoccupied. On

the other hand, all the eight vacancy sites are filled with pre-adsorbed oxygen molecules for the high O₂ case, while the remaining four oxygen molecules were randomly adsorbed near five-fold surface tin cations. All the adsorbed oxygen molecules at oxygen vacancy sites were assigned partial charges equivalent to those calculated for the O⁻² adsorbed on the reduced (101) surface, while those adsorbed at Sn_{5c} sites were kept neutral to imitate their weak physisorption on stoichiometric sites.

The trajectories of acetone and ethanol molecules indicate that they gradually move towards the SnO₂ surface as the MD simulation proceeds. Typically, most of the molecules are adsorbed on the surface within 30 ps, and hence the simulated period of 100 ps is enough to ensure that all the molecules are stabilized in their positions. For the low O₂ scenarios (Figure S5-a, b), we observe that four acetone (or ethanol) molecules first adsorb at the un-occupied oxygen vacancy locations, while the four remaining molecules directly bind to a surface Sn_{5c} resembling the adsorption on a stoichiometric surface. On the other hand, for the high O₂ scenarios where all vacancy sites are taken (Figure S5-c, d) acetone (or ethanol) molecules either share a vacancy site with a pre-adsorbed oxygen molecule, or directly bind to a surface Sn_{5c}. Moreover, we notice that the remaining neutral oxygen molecules physisorbed on the surface desorb back to the vacuum space after the adsorption of ethanol and acetone, indicating their weak binding as compared to the chemisorbed O⁻² species that exhibit strong electrostatic interaction with the surface.

By analyzing the potential energy of the system over time, we observe that the system typically reaches a minimized energy state within 30-40 ps from the start of the simulation, which indicates that all the molecules could find their most stable configurations on the surface. Moreover, by inspecting the components of the potential energy of the system, we noticed that the electrostatic interactions are dominant over vdW forces. This confirmed the key role played by the specific interactions of polar groups, such as the hydroxyl group of ethanol and the carbonyl group of acetone, in their adsorption on metal oxide surfaces.

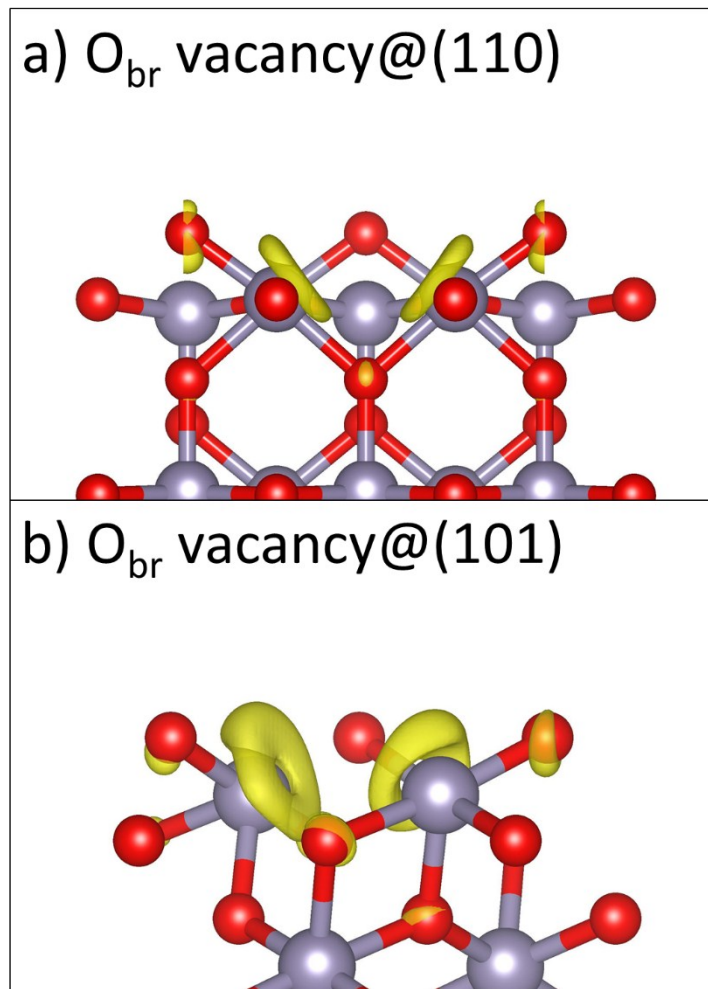


Figure S1. Charge density deformation due to bridging oxygen vacancy formation at the (110) and (101) surfaces of SnO₂.

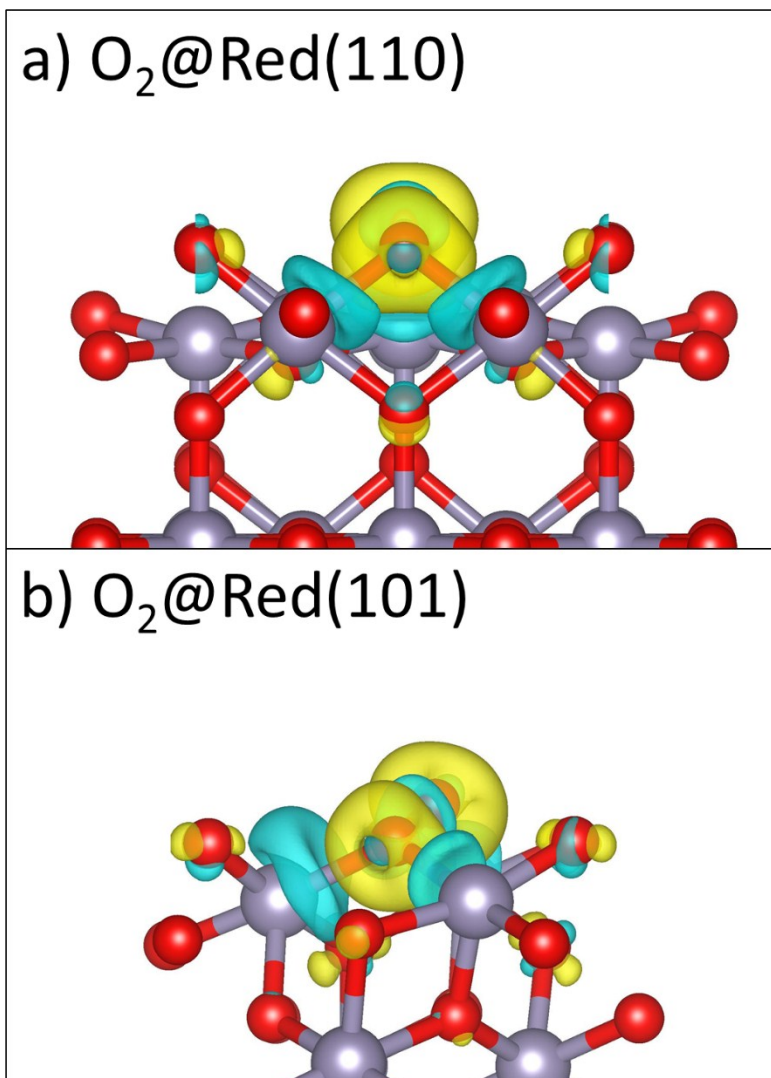


Figure S2. Charge density deformation of oxygen adsorption on the reduced (110) and (101) surfaces of SnO_2 .

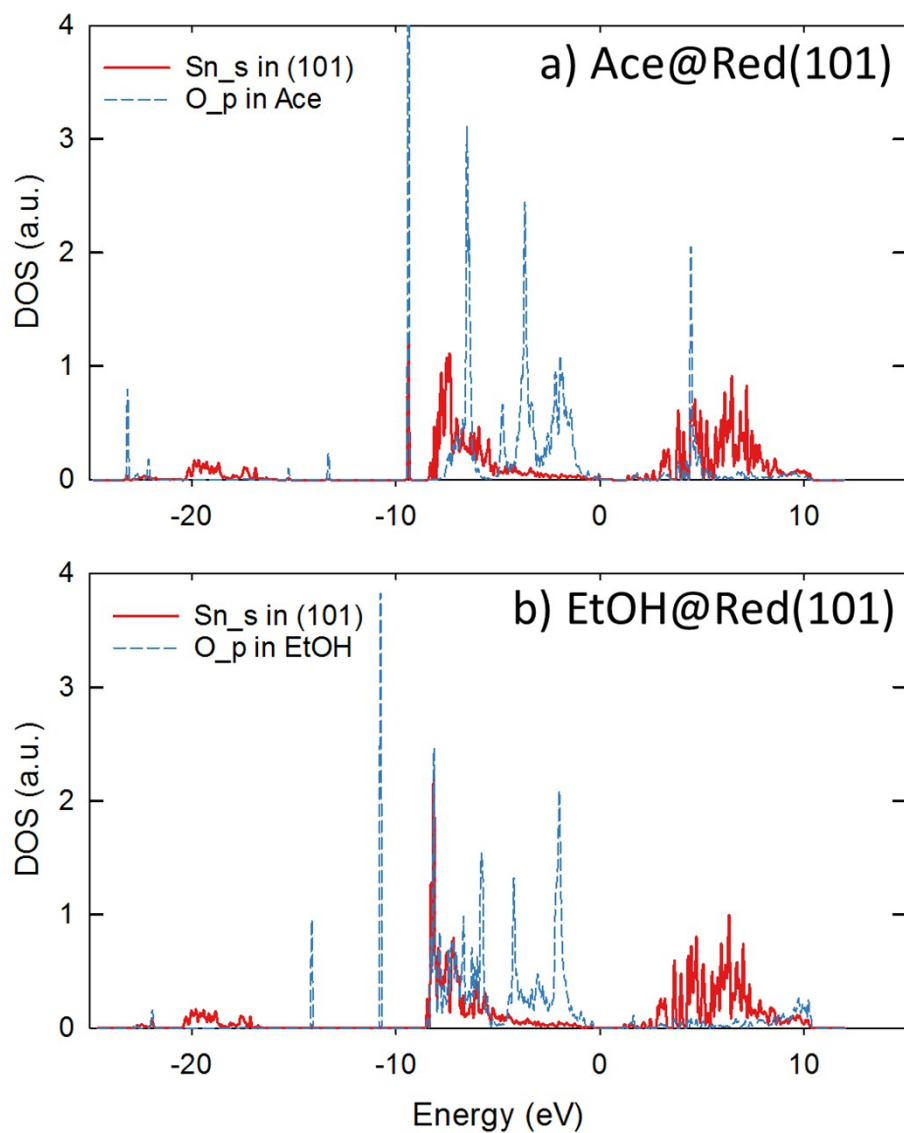


Figure S3. Projected density of states of the Sn-5s orbital for the surface Sn cation adjacent to the bridging oxygen vacancy, and the O-2p orbital of the O_{Ace} and O_{EtOH} after the adsorption of acetone and ethanol.

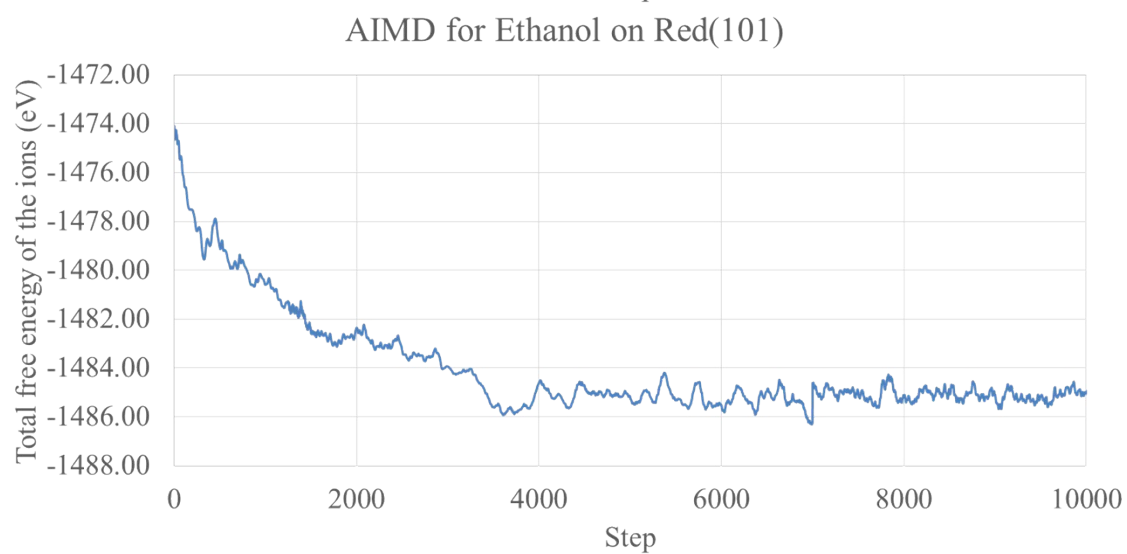
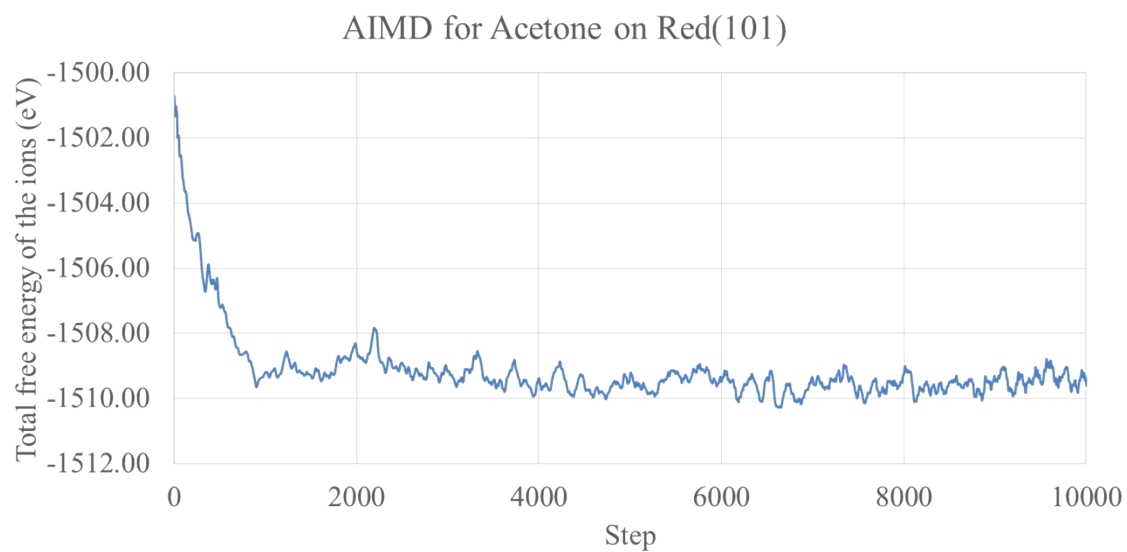


Figure S4. Total energy change during AIMD simulations

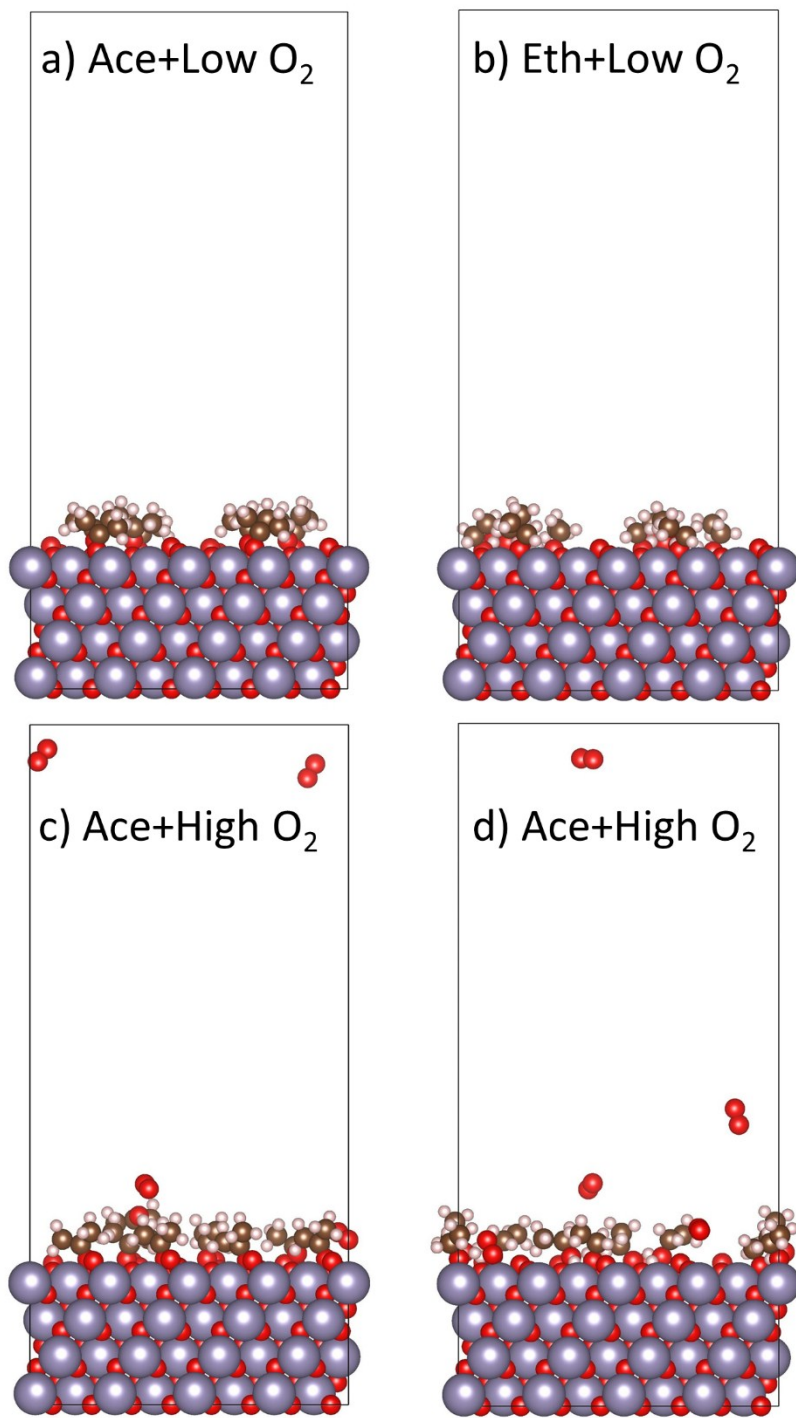


Figure S5. FF-MD simulation results